Cancer Chemother Pharmacol (2008) 61:727–737
DOI 10.1007/s00280-007-0527-3

ORIGINAL ARTICLE

Potentiation of arsenic trioxide cytotoxicity by Parthenolide and buthionine sulfoximine in murine and human leukemic cells

Markus Duechler · Małgorzata Stańczyk · Małgorzata Czyż · Maciej Stępnik

Received: 12 March 2007 / Accepted: 11 May 2007 / Published online: 27 June 2007

Abstract
Purpose To possibly increase the in vitro cytotoxic activity of arsenic trioxide (ATO) by combining it with Parthenolide (PRT), a known NF-κB inhibitor and buthionine sulfoximine (BSO), an inhibitor of γ-glutamylcysteine synthetase.
Methods Several cell lines representing various hematological malignancies were treated in vitro with the study drugs alone or in combinations. Flow cytometry was used to assess cell death rates and reative oxygen species production. Glutathione and ATP levels were determinded using a photometric and a luminometric assay, respectively. Cell death was characterised by fluorescence microscopy and DNA fragmentation analysis.
Results PRT increased cytotoxicity of ATO in seven out of eight cell lines. Addition of buthionine sulfoximine (BSO) further potentiated cytotoxicity of the combined treatment. When combined with PRT and BSO, clinically achievable concentrations of ATO (2.5 μM) induced cytotoxicity rates of 80–98% after 24 h. Importantly, lymphocytes from healthy donors were largely unaffected by these treatment modalities, also after growth stimulation in cell culture. *N*-acetylcysteine inhibited the cytotoxic effects of the triple combination. Treatment of leukemic cells with ATO, PRT and BSO rapidly depleted cells from glutathione, induced oxidative stress and decreased intracellular ATP levels. Cell death showed characteristics of necrosis presumably as a result of ATP loss.
Conclusion Based on the observed selectivity towards malignant cells this combination may offer a therapeutic option applicable to different kinds of leukemia.

Keywords Arsenic trioxide · Parthenolide · Buthionine sulfoximine · Leukemia therapy · Necrosis

Introduction

Arsenic has played a significant therapeutic role in various diseases for over 2,000 years. In the 1990s, reports by Chinese investigators, of the considerable activity of arsenic trioxide (ATO), against acute promyelocytic leukemia, raised the hopes for the potential use of this drug in treatment of other forms of leukemia as well [28]. The activity of ATO was consecutively investigated in several types of hematologic malignancies [34]. The clinical effects of these trials were not as spectacular as those observed in APL. The cytotoxic efficacy of ATO against hematologic malignancies may be enhanced by blocking ATO-induced stress response of cancer cells which include upregulation of the anti-apoptotic transcription factor NF-κB and an increase of intracellular glutathione levels.

NF-κB regulates transcription of a great diversity of genes involved in inflammatory responses, cell growth and apoptosis [16]. Many neoplastic cells of hematologic origin and solid tumors show abnormal NF-κB activation, which contributes to hyperproliferation, resistance to apoptosis, and disease progression [1, 33]. Pharmacological inhibition

M. Duechler (✉) · M. Stańczyk · M. Stępnik
Department of Toxicology and Carcinogenesis,
Nofer Institute of Occupational Medicine,
8 Sw. Teresy Street, 91-348 Łódź, Poland
e-mail: markusd@imp.lodz.pl

M. Czyż
Department of Molecular Biology of Cancer,
Medical University of Łódź, 6/8 Mazowiecka Street,
92-215 Łódź, Poland

of NF-κB has been demonstrated to increase the proapoptotic effect of ATO [31]. Arsenic itself either stimulates [7, 36] or inhibits [17, 19, 22] NF-κB activity depending on the cell type, the concentration used, as well as intracellular glutathione (GSH) and H_2O_2 levels [12, 38]. At concentrations higher than 10 μM, ATO inhibits NF-κB activity by interacting with a specific cysteine residue in the activation loop of the IκB kinase (IKK) catalytic subunits [15]. ATO generates reactive oxygen species (ROS) which contribute to cell death induction [2] and at lower concentrations may stimulate NF-κB activity [7].

Many reports suggest that the sensitivity of leukemic cells to ATO correlates with their intracellular GSH levels [37, 41]. Cell lines or their clones expressing higher levels of GSH and GSH-associated enzymes are less sensitive to ATO than cells expressing low levels of these molecules. GSH seems to have two functions with respect to ATO toxicity: it is part of a detoxification system which removes ATO from the cell; and it protects cells from reactive oxygen species which are produced upon exposure to ATO. Cells can be sensitised to ATO cytotoxic effects by agents that deplete intracellular GSH [3, 5, 13] not only in leukemic cells but also in solid tumors [21, 27].

In our present study, two cellular anti-apoptotic responses were inhibited simultaneousley to increase the cytotoxicity of arsenic trioxide. Parthenolide (PRT), a known NF-κB inhibitor [18] and buthionine sulfoximine (BSO), an irreversible inhibitor of γ-glutamylcysteine synthetase were used to shut down NF-κB activity and to reduce intracellular GSH levels, respectively. The effect of combined treatment was evaluated on selected murine (EL-4) and human leukemia cell lines (Jurkat, K562 and HL-60). Cytotoxicity of combinations of ATO, PRT and BSO was evaluated in vitro on the leukemic cell lines and compared to healthy donor lymphocytes. Changes in reactive oxygen species (ROS) production, GSH levels and ATP content were assessed. Cell death was characterised by evaluating several apoptotic parameters. The combined treatment showed selective cytotoxicity towards leukemic cells and might provide a promising therapeutic approach.

Materials and methods

Chemicals

Arsenic trioxide (ATO), propidium iodide and 2′,7′-dichlorodihydrofluorescein diacetate (DCF) were obtained from Fluka (Sigma–Aldrich, St. Louis, MO, USA). Camptothecin, z-VAD-fmk, L-N-acetylcysteine (NAC), alpa-Tocopherol, L-Buthionine-sulfoximine (BSO), Annexin V-FITC Apoptosis Detection Kit, the Glutathione Assay Kit and 4′-6-Diamidino-2-phenylindole (DAPI) were from from Sigma Chemical Company (Sigma–Aldrich, St. Louis, MO, USA). Phytohemagglutinine (PHA) was from Calbiochem (Merck, Darmstadt, Germany). The ATP determination kit was purchased from Molecular Probes (Invitrogen Corporation, San Diego, CA).

Cell culture

EL-4 mouse thymoma cells were cultured in DMEM, 10% fetal bovine serum (FBS), 2 mM glutamine and antibiotics (penicillin 100 U/ml and streptomycin 100 μg/ml). Jurkat T cells, K562 erythroleukemia cell line, and HL-60 promyelocytic cells were grown in RPMI 1640 medium containing glutamine complemented with 10% FBS and antibiotics. Lymphocytes were isolated from healthy volunteers (HDL) by Ficoll centrifugation and cultured in RPMI medium containing glutamine, 20% FBS, and antibiotics. For growth stimulation, PHA was added to a final concentration of 10 μg/ml. The Burkitts Lymphoma cell lines BL41 and Ramos, the B-cell chronic lymphocytic leukemia cell line MEC-1 and the precursor B-cell line REH, were grown in RPMI 1640 medium with 10% FBS, 2 mM glutamine and antibiotics. EL-4 cell line (originally from ATCC) was kindly provided by J. Dastych, all other cell lines used were purchased from DSMZ (Braunschweig, Germany).

Assessment of cell viability

Cell viability was assessed based on propidium iodide (PI) staining. After incubation with drugs in complete culture medium for 24 h at a cell density of 0.25–0.5 × 10^6 cells/ml, cells were washed once in phosphate-buffered saline (PBS) and resuspended in 0.25 ml of 2 μg/ml PBS/PI solution. After 10 min of staining [room temperature (RT), in the dark] cell fluorescence was measured by flow cytometry. PI-negative cells were defined as viable. Flow cytometric analysis was performed on a Cytomics FC500 MPL cytometer from Beckman Coulter (Fullerton, CA). Data were analysed using the CPX software package.

Measurement of reactive oxygen species production

Intracellular ROS levels were visualised after incubation with 2′,7′-dichlorodihydro-fluorescein diacetate (DCF) at a final concentration of 10 μM. The fluorescent dye was added for the last 30 min of the drug exposure period. After the incubation cells were washed once in PBS, resuspended in PBS and examined immediately by flow cytometry.

Assessment of intracellular ATP level

Changes in intracellular ATP content were measured using a bioluminescence assay with recombinant firefly luciferase and its substrate D-luciferin. After the drug incubations, cells were harvested by centrifugation, washed once with PBS and lysed in 1% TCA (trichloroacetic acid) by two freeze thawing cycles. ATP content was determined in the supernatant after centrifugation. The light produced in the reaction of luciferin with ATP was detected in a luminometer (Fluoroskan Ascent FL, Labsystems, Helsinki, Finland).

Measurement of intracellular GSH content

Changes in total cellular gluthathione levels were determined using a "Glutathione Assay Kit" following the included instructions. (1–5) $\times 10^7$ cells were used for each sample. Briefly, cells were lysed by freeze/thawing and protein was precipitated with 5% 5-sulfosalicylic acid (SSA) solution. GSH in the supernatant was quantified by its ability to convert 5,5′-dithiobis(2-nitrobenzoic acid) into the yellow product 2-nitrobenzoic acid which was measured spectrophotometrically.

AnnexinV staining procedure

Cells were harvested by centrifugation, washed once with PBS and incubated at a density of 1×10^6 cells/ml with fluorescein-labelled Annexin V (0.5 μg/ml) and propidium iodide (PI, 2 μg/ml) in binding buffer (10 mM HEPES pH 7.5; 140 mM NaCl; 2.5 mM $CaCl_2$). After 15 min at RT in the dark fluorescence was assessed by flow cytometry. Late apoptotic/necrotic cells have disrupted membranes and stain positive for both, Annexin V and PI, while early apoptotic cells with externalised phosphatidylserine appear as Annexin V single positive population.

Cell cycle analysis

Cells were harvested by centrifugation, washed once in PBS and fixed with 70% ethanol at −20°C overnight. Cells were washed again with PBS and resuspended in PBS containing 0.1% Triton-X100, 200 μg/ml RNaseA and 20 μg/ml PI. After incubation for 15 min at RT in the dark relative DNA content was measured by flow cytometry.

Detection of nuclear fragmentation

After drug incubations cells were collected by centrifugation, resuspended in PBS containing 0.2 μg/ml DAPI and visualised in a fluorescence microscope. Using this method, only nuclei of damaged cells are stained. Fragmented nuclei are characteristic of apoptotic cells, while stained intact nuclei indicate necrotic cells.

DNA fragmentation analysis

Low molecular weight DNA was extracted from cells by the method of Gong et al. [10] with slight modifications. Briefly, 2×10^6 cells were washed in cold PBS after drug treatment for 24 h and fixed in ice-cold 70% ethanol overnight. The fixed cells were resuspended in 40 μl extraction buffer (0.2 M phosphate–citrate buffer, pH 7.8) and incubated at room temperature for 30 min. After centrifugation the supernatants containing low molecular weight DNA were dried, resuspended in 3 μl 0.25% NP-40 and incubated with 3 μl DNase-free RNase A (1 mg/ml) at 37°C for 30 min. Next, 3 μl Proteinase K (1 mg/ml) were added and samples were further incubated at 37°C for 40 min. After incubation, the samples were subjected to agarose gel electrophoresis. With this method no DNA is isolated from intact cells, fragmented DNA is extracted from apoptotic cells, while high molecular weight DNA is typically derived from necrotic cells.

Statistical analysis

All measurements of cytotoxicity, ROS, GSH and ATP were done in triplicates, and at least three independent experiments were done unless stated differently. Data are shown from one typical experiment and expressed as mean of triplicates ± SE. Statistical analysis was performed using Student's *t*-test. Differences were considered significant if $P < 0.05$ (marked by asteriks).

Results

PRT enhanced ATO-mediated cytotoxicity

The influence of PRT on arsenic-mediated cytotoxicity was investigated in EL-4 murine thymoma cells, Jurkat human T cells, HL-60 human promyelocytic cells, and K562 human erythroleukemic cells. Cells were incubated for 24 h with increasing concentrations of ATO (2.5–10 μM) alone or in combination with PRT. PRT in the combinatorial treatments was kept constant at 10 μM. This concentration was chosen based on earlier experiments in which the cytotoxicity of PRT was measured (not shown). PRT at 10 μM resulted in about 15% dead cells in the most sensitive cell line (Jurkat) and less than 10% in the other cell lines tested. As shown in Fig. 1a, PRT-enhanced cytotoxicity of ATO in EL-4, Jurkat and HL-60 cells, while K562 cells were refractory to ATO and the combinatorial treatment.

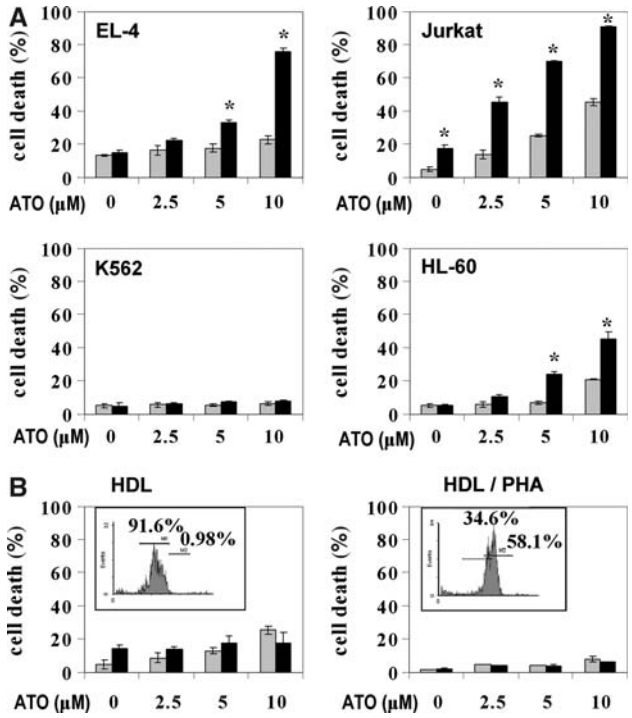

Fig. 1 Cytotoxicity of the combined application of ATO and PRT. Cells were incubated for 24 h with 0, 2.5, 5 or 10 μM ATO alone (*grey bars*) or together with 10 μM PRT (*black bars*). Cytotoxicity was measured by propidium iodide (PI) staining and flow cytometry. The percentage of dead cells is shown for **a** EL-4, Jurkat, K562, and HL-60, or **b** healthy donor lymphocytes. HDL ($n = 6$) were either exposed to drugs immediately (*left diagram*) or cultured for 24 h in the presence of 10 μg/ml PHA before addition of drugs (*right diagram*). Stimulation of DNA synthesis was assessed by cell cycle analysis after staining with PI (*inset*). *, $P < 0.05$, compared to ATO alone

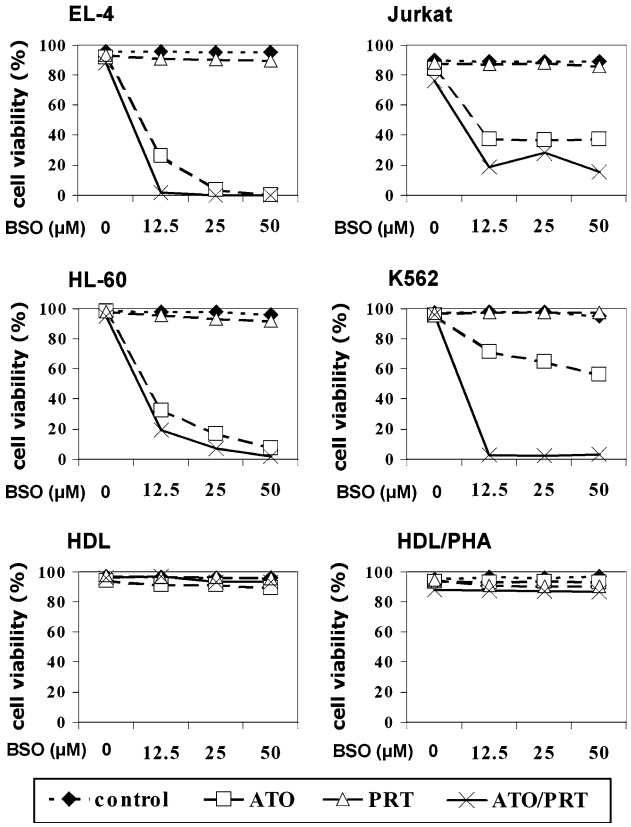

Fig. 2 Increased cytotoxic effects of ATO–PRT combinations by addition of BSO. Cell viability was measured after 24 h of incubation with 2.5 μM ATO, 10 μM PRT, or the combination of both, together with increasing concentrations of BSO. Cell viability was assessed by PI staining, the percentage of viable cells measured in triplicates from one typical experiment is shown. Standard deviations are omitted from the figure for better clarity; their values were <7% at all points

Healthy donor lymphocytes (HDL) were resistant to the combinatorial treatment

PRT alone caused cell death of about 10% in lymphocytes isolated from the blood of healthy volunteers (n = 6). Arsenic treatment showed a dose-dependent cytotoxic effect reaching ~25% dead cells at 10 μM ATO, in good agreement with published results [11]. Co-incubation with PRT did not further increase cell death (Fig. 1b). To explore whether the lower sensitivity of HDL was related to their resting status, part of the cells were growth stimulated with phytohemagglutinin (PHA) for 24 h and the culture was continued for another 24 h in the presence of drugs. Entry into S-phase was shown by cell cycle analysis. In a typical example, the percentage of cells in S-phase increased from 1% (unstimulated) to 58% in the stimulated culture (see inset in Fig. 1b). No difference in the sensitivity to drug treatment was observed in growth-stimulated HDL as compared to resting cells.

BSO further increased the cytotoxic effects of ATO and the ATO–PRT combination

To investigate the impact of intracellular glutathione levels, we assessed the cytotoxicity of ATO, PRT and their combinations after GSH depletion by BSO. BSO increased the cytotoxicity of ATO in all cell lines (Fig. 2). Addition of 12.5 μM BSO to the ATO–PRT combination raised cytotoxicity rates to 80–98% after 24 h in EL-4, Jurkat, K562 and HL-60 cells. Note, that application of the single drugs at the concentrations used in the triple combination caused <10% dead cells (Fig. 2, 0 μM BSO). Remarkably, K562 cells also, which were resistant to ATO–PRT, were efficiently killed when BSO was added. In contrast, lymphocytes isolated from the blood of healthy donors ($n = 6$) were fairly well resistant to the same treatment. Incubation with drug combinations which killed 80–98% of malignant cells induced cell death in less than 10% of HDL. Again, stimulated and unstimulated HDL showed no differences in drug sensitivity. When the incubation time was prolonged

to 48 h, a triple combination consisting of 2.5 μM ATO, 10 μM PRT and 12.5 μM BSO resulted in 15–35% dead HDL ($n = 3$, data not shown).

Four additional human leukemic cell lines were tested for their sensitivity to the combined treatment including the Burkitts Lymphoma cell lines BL41 and Ramos, MEC-1 (B-cell chronic lymphocytic leukemia), and REH (B-cell precursor). In all cases more than 85% of cells were killed by the ATO–PRT–BSO combination after 24 h (Table 1).

ATO and PRT increased intracellular GSH levels

The influence of BSO, ATO and PRT on intracellular GSH content was first examined after 24 h. As expected, BSO depleted cells from GSH in all cell lines tested (Table 2). Treatment with ATO, PRT or their combination raised intracellular GSH content relative to untreated cell cultures (Table 2). The maximum increase in GSH level in response to ATO was about 5-fold in EL-4 (10 μM), 3.6-fold in HL-60 (2.5 μM) and 2-fold in K562 (5 μM). The maximal increase observed in Jurkat cells was only about 1.5-fold (2.5 μM).

The relative increase of the intracellular GSH level following drug treatment was inversely related to the sensitivity to ATO-mediated killing. Among the three cell lines responsive to ATO, Jurkat cells showed the smallest relative increase in GSH and the highest cytotoxic rate after exposure to ATO. EL-4 and HL-60 cells had lower steady state levels in untreated cells than Jurkat, but responded with a more pronounced GSH increase (Table 2) and less dead cells after ATO exposure (Fig. 1).

Drug treatment increased intracellular levels of reactive oxygen species

An increase in ROS levels is thought to constitute an essential step in cell death induction by arsenicals [38, 14]. To assess intracellular ROS levels, cells were labelled with dichloro-dihydrofluorescein-diacetate (DCF) and fluorescence was measured by flow cytometry. Figure 3 shows the influence of drug treatment on DCF fluorescence during the first 12 h. In EL-4 and HL-60 cells, ATO alone and its combination with PRT or BSO increased ROS levels. For the ATO–PRT–BSO triple combination, increases in ROS levels were observed in all cell lines ranging from 1.2-fold (K562) to 3-fold (HL-60) relative to control cells. ROS levels were elevated during the first 6 h but were back at control levels (EL-4) or below after 12 h.

Table 2 Glutathione content after 24 h

	EL-4	Jurkat	K562	HL-60
Control	2.6 ± 0.04	10.4 ± 0.51	7.6 ± 0.47	2.5 ± 0
ATO 2.5 μM	6.9 ± 0.14	15.4 ± 0.16	14.9 ± 0.08	9.1 ± 0.25
ATO 5 μM	9.6 ± 0.24	14.7 ± 0.98	15.9 ± 0.31	8.1 ± 0.35
ATO 10 μM	13.4 ± 0.29	12.9 ± 0.30	12.6 ± 0.28	7.9 ± 0
PRT 10 μM	4.3 ± 0.13	11.0 ± 2.33	22.1 ± 0.41	3.7±0.32
ATO + PRT	7.5 ± 0.19	16.5 ± 2.48	27.6 ± 1.52	9.0 ± 0.02
BSO 12.5 μM	0.7 ± 0.03	3.0 ± 0.03	1.0 ± 0	0.6 ± 0.45

EL-4, Jurkat, K562 and HL-60 cells were incubated with ATO, PRT (10 μM), ATO + PRT (2.5 μM + 10 μM), or BSO. After 24 h cells were counted, harvested, and lysed by freeze/thawing in 5% SSA. GSH content was determined and is expressed in nmol per 10^6 cells

N-acetylcysteine, but not alpha-Tocopherol reduced the cytotoxic effect

To further investigate the importance of ROS the influence of *N*-acetylcysteine and alpha-Tocopherol was evaluated. Addition of 5 mM NAC protected EL-4 cells from the cytotoxic effects of the ATO–PRT–BSO combination (Fig. 4). Similar results were obtained for Jurkat, K562 and HL-60 cell lines (not shown). NAC also inhibited the cytotoxic effect of ATO, PRT and their combinations. In contrast, alpha-Tocopherol at a concentration of 0.1 mM did not show any protecting effect in EL-4 (Fig. 4), K562 and Jurkat cells, and a moderate inhibition of cell death (<30%) in HL-60 cells (not shown).

During ATO–PRT–BSO-induced cell death the late steps of apoptosis were prohibited

To evaluate the mechanism underlying cell death, four different methods (a–d) were applied; (a) Externalisation of phosphatidylserine in the plasma membrane was monitored

Table 1 Cell viability of leukemic cell lines after 24 h

	Control	ATO	PRT	ATO + PRT	ATO + BSO	ATO + PRT + BSO
BL-41	94.4 ± 0.4	76.8 ± 0.6	79.1 ± 1.8	29.2 ± 1.6	23.1 ± 3.1	12.8 ± 0.6
MEC-1	98.4 ± 0.2	89.4 ± 0.5	54.2 ± 0.5	7.9 ± 1.7	52.3 ± 3.1	5.7 ± 0.5
Reh	97.8 ± 0.1	81.8 ± 3.2	72.9 ± 1.0	5.1 ± 0.6	8.7 ± 0.6	14.7 ± 1.7
Ramos	98.3 ± 0.2	89.4 ± 1.0	76.6 ± 0.8	27.7 ± 0.4	4.8 ± 0.8	4.3 ± 1.8

Cells were incubated for 24 h with drug combinations as indicated. The concentrations used were 2.5 μM ATO, 10 μM PRT and 12.5 μM BSO. Cell viability was assessed by propidium iodide staining and flow cytometry

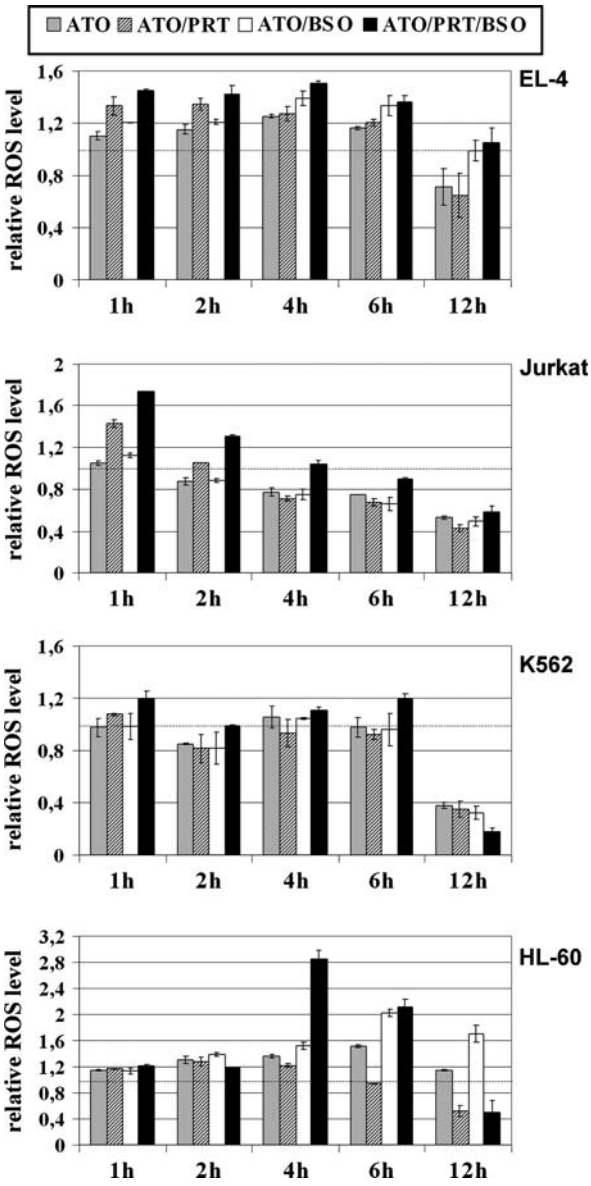

Fig. 3 Production of reactive oxygen species (ROS) in drug-treated cells. EL-4, Jurkat, K562, or HL-60 cells were incubated for 1, 2, 4, 6 and 12 h with various combinations of ATO, PRT and BSO (2.5, 10 and 12.5 μM, respectively) as indicated. DCF at a concentration of 10 μM was added to cell cultures during the last 30 min of incubation. Cells were washed in PBS and green fluorescence was measured by flow cytometry. The mean fluorescence intensity was used as read-out for intracellular ROS levels

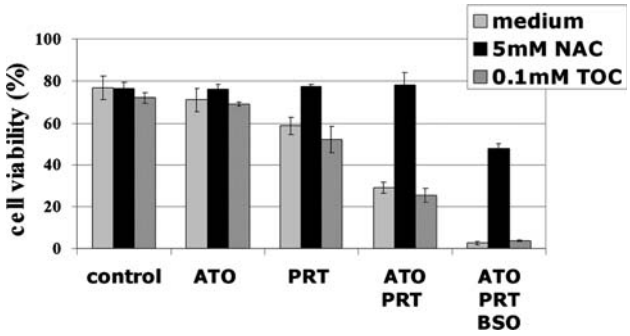

Fig. 4 Inhibition of the cytotoxic effect of drug treatment by *N*-acetylcysteine. EL-4 cells were incubated for 24 h with 10 μM ATO, 20 μM PRT, the combination of 5 μM ATO with 20 μM PRT, or 2.5 μM ATO with 10 μM PRT and 12.5 μM BSO. In parallel experiments, either *N*-acetylcysteine (5 mM) or alpha-Tocopherol (0.1 mM) was added. Cell viability was measured after PI staining by flow cytometry, the percentage of viable cells is shown

by binding of Annexin V (labelled with fluoresceine). After 20 h of drug treatment a clear population of Annexin single-positive cells was detected as shown in Fig. 5a for Jurkat cells. A similar picture was obtained for EL-4 and HL-60 cells, while K562 did not show Annexin V single-positive cells. (b) The involvement of caspases was explored by their inhibition with the pan-caspase inhibitor z-VAD-fmk. As shown in Fig. 5b, cell death induction by the triple drug combination was substantially inhibited only in Jurkat cells, demonstrating that activation of caspases was not critically required for cell death induction in the other cell lines. (c) In the late stage of apoptosis, cells show a typical pattern of nuclear fragmentation, which was examined by staining whole cells with DAPI without fixation and permeabilisation. In the first panel of Fig. 5c, Camptothecin-treated EL-4 cells are shown which display typical pictures of fragmented apoptotic nuclei. When Camptothecin-mediated apoptosis was blocked by inhibition of caspases with z-VAD-fmk, no nuclear fragmentation was visible (Fig. 5c, lower panel, left picture). ATO induced a mixture of apoptotic and necrotic cells, whereas PRT or the combination of arsenic and PRT showed mainly apoptotic cells (Fig. 5c, upper panel). The addition of BSO prevented nuclear fragmentation (Fig. 5c, lower panel). This effect was most pronounced in EL-4 cells, but also clearly visible in HL-60 and Jurkat cells (not shown). K562 cells did not show any fragmented nuclei in agreement with its reduced ability to undergo apoptosis (not shown).

(d) Finally, DNA fragmentation was assessed to further differentiate between apoptotic and necrotic cell death. DNA extracted from EL-4 cells showed apoptotic DNA laddering after treatment with 5 μM Camptothecin, 2.5 μM ATO, 10 μM PRT or the combination of both (Fig. 5d). In contrast, DNA fragmentation was almost absent after incubation with 10 μM ATO or with combinations of ATO and BSO. Instead, high molecular DNA, typical of necrotic cells was observed under these treatment conditions. Similar results were found in HL-60 and Jurkat cells (not shown).

Taken together, our results from these four measurements suggested that in the cell death program induced by the combination of ATO and BSO the early steps of apoptosis like externalisation of phosphatidylserine still took

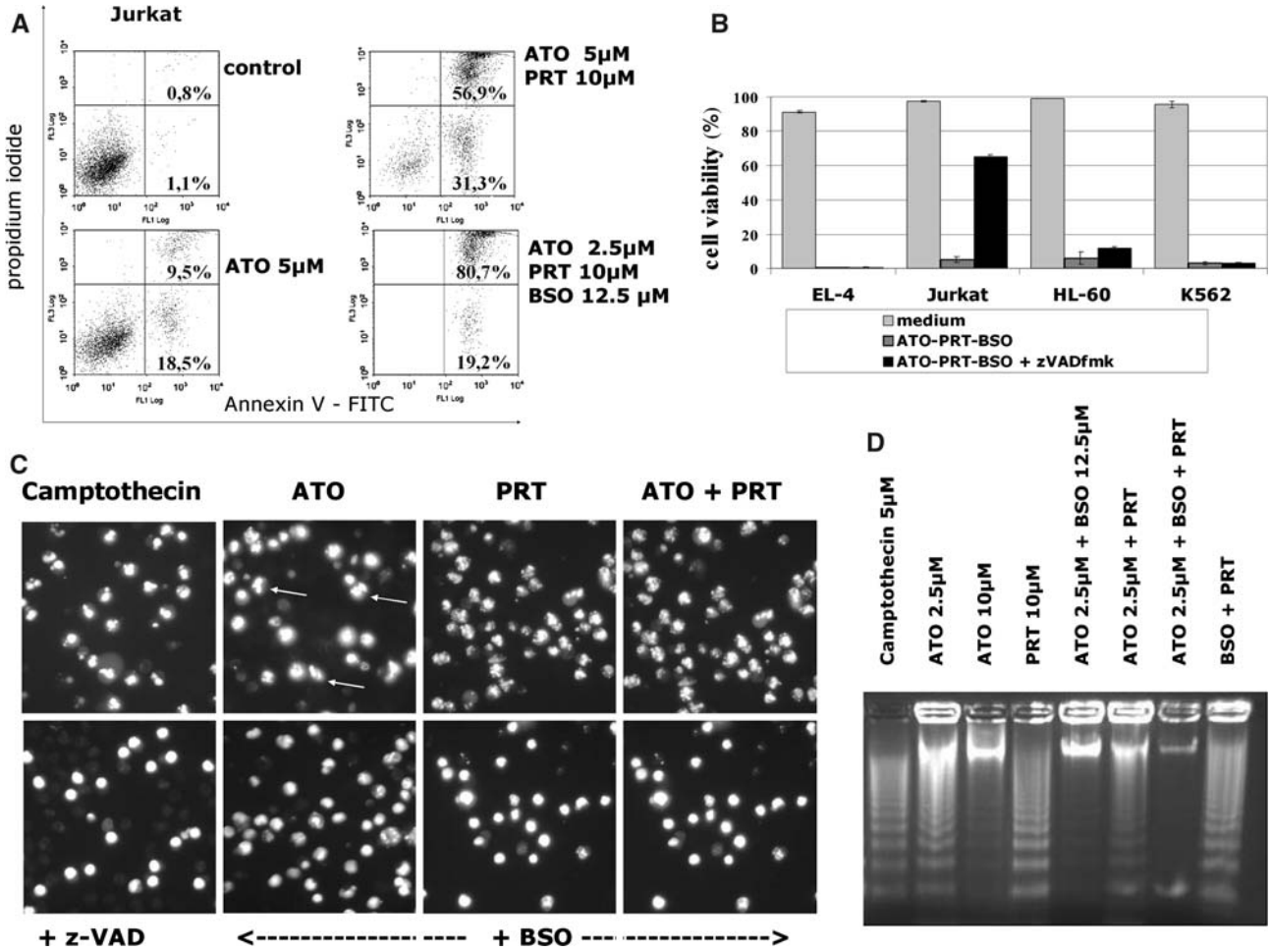

Fig. 5 Assessment of apoptotic and necrotic parameters. **a** Jurkat cells were incubated for 20 h with drugs as indicated. Staining with Annexin V and propidium iodide revealed Annexin V single-positive apoptotic cell populations. **b** The dependence of cell death induced by ATO–PRT–BSO on caspase activity was tested. Cells of the four lines tested were incubated for 24 h with a drug combination consisting of 2.5 µM ATO, 10 µM PRT and 12.5 µM BSO in the presence or absence of 20 µM zVADfmk. Cell viability was determined by PI staining and flow cytometry. *, $P < 0.05$ compared to incubation without zVADfmk. **c** The number of fragmented nuclei of apoptotic cells was reduced in combinations containing BSO. EL-4 cells were cultivated for 24 h with 5 µM Campthotecin, 5 µM ATO, 20 µM PRT, or a combination of 5 µM ATO and 10 µM PRT. In the lower panel, either the pan-caspase inhibitor z-VADfmk (20 µM) or 12.5 µM BSO was added as indicated. In the picture showing ATO-treated cells some apoptotic nuclei are indicated by arrows. **d** EL-4 cells were treated for 24 h with drug combinations as indicated. DNA was extracted and subjected to agarose gel electrophoresis. Camptothecin treated cells (5 µM) were used as positive control for apoptotic DNA laddering

place, while late steps of apoptosis including nuclear condensation and DNA fragmentation were prohibited. These observations indicated that during drug incubation the cell death mechanism was shifted towards necrotic cell death.

Drug treatment reduced intracellular ATP levels

To determine whether depletion of intracellular ATP caused the switch from energy-dependent apoptosis to necrotic cell death, ATP content was assessed in the four cell lines treated with drug combinations for 2–12 h. Incubation with ATP-PRT-BSO induced a drop of ATP levels to 50% or less after 6 h and to 25% or less after 12 h in EL-4, Jurkat and HL-60 cells lines. In K562 cells ATP levels were reduced at the same time point by about 30% of control values (Fig. 6).

Intracellular GSH levels dropped dramatically during the initial phase of drug treatment

BSO at 12.5 µM depleted the cells from GSH after 24 h (Table 2), but did not induce apoptosis per se. Reactive oxygen species supposed to trigger cell death peaked during the first 6 h but were back at control levels or even below after 12 h. To investigate whether the oxidative stress during the first 6 h would meet reduced GSH levels in our experiments, we assessed intracellular GSH levels during the first 12 h of drug incubation (Fig. 7). As

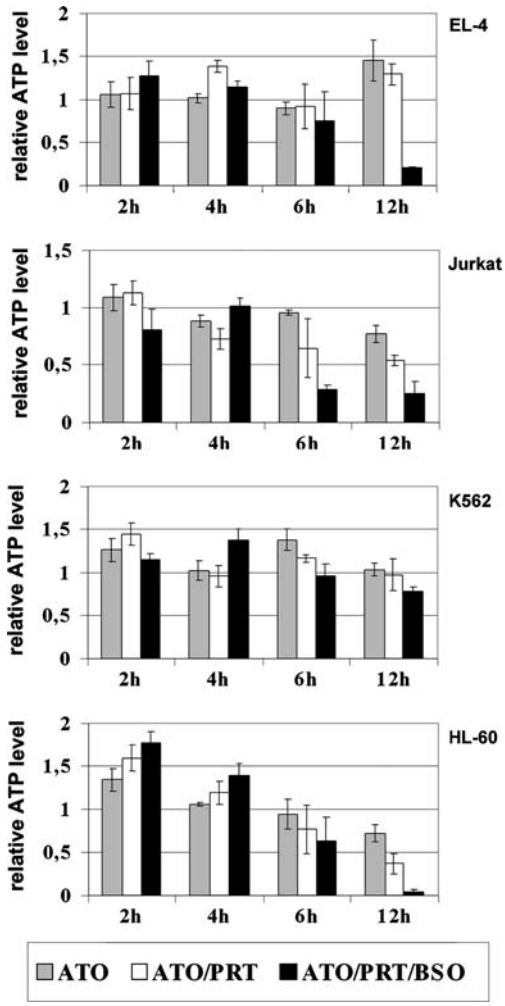

Fig. 6 Changes of intracellular ATP content during drug treament. Cells were treated with 5 μM ATO, 2.5 μM ATO + 10 μM PRT, 2.5 μM ATO + 12.5 μM BSO, or 2.5 μM ATO + 10 μM PRT + 12.5 μM BSO for 2, 4, 6 and 12 h. ATP was determined in a luminometric assay based on oxidation of luciferin by firefly luciferase in an ATP-dependent reaction. Results are shown relative to untreated controls

expected, incubation with BSO slowly decreased GSH content and this decrease was accelerated in the presence of ATO. The analysis also confirmed that ATO alone and the ATO–PRT combination increased GSH levels. Strikingly, incubation with the triple combination resulted in a very rapid loss of GSH in all cell lines. In Jurkat, K562 and HL-60 cells a significant decrease was visible already after 1 h and reached more than 50% after 2 h (Fig. 7). After 12 h all cell lines including EL-4 were almost completely exhausted from GSH.

Discussion

The successful treatment of acute promyelocytic leukemia with arsenic trioxide stimulated a steadily increasing number of in vitro studies and clinical trials in order to realise its practicability in cancer therapy. In the current study we demonstrate increased cytotoxic activity of ATO in combination with PRT and BSO. It has been previously reported that either inhibition of NF-κB or lowering cellular GSH level increased ATO toxicity [3, 31, 42]. PRT is a well-known inhibitor of NF-κB, but has other anti-cancer effects as well. In multiple myeloma cells and B-cell chronic lymphocytic leukemia cells, PRT-induced apoptosis included ROS generation [29, 35]. In colorectal cancer cells, PRT was described to rapidly deplete cells from GSH and protein thiols, concomitant with an increase in ROS levels [40], and to induce sustained activation of JNK independent from NF-κB inhibition [23, 39]. Therefore, PRT might have other effects in addition to NF-κB inhibition.

The application of the ATO–PRT–BSO triple combination resulted in high death rates in all cell lines tested, including murine EL-4 thymoma cells, and several human cell lines of myeloid and lymphoid origin. Cytotoxic rates of 80–98% were obtained during the first 24 h. Importantly, healthy donor lymphocytes were quite resistant to the same treatment, which killed most leukemic cells. The rapid cell death induction in leukemic cells by the triple combination raises the hope that a short treatment with low overall toxicity may be sufficient to eradicate leukemic cells in patients, too.

The cytotoxic effects of ATO–PRT–BSO could be largely inhibited by NAC underlining the importance of the thiol status for the sensitivity to cell death induction by this combination. Treatment with ATO alone or the combination of ATO and PRT resulted in increased GSH levels indicating an antioxidant response to those drugs. We observed that the strength of this antioxidant response determined the susceptibility of a cell line to ATO-induced cell death rather than the steady-state levels of GSH in untreated cells.

Depletion of GSH by BSO alone did not reduce cell viability but oxidative stress caused by ATO and/or PRT might be the actual trigger for cell death induction [38, 14]. Elevated ROS levels were measured in EL-4, Jurkat and HL-60 cells during the first 4–6 h after ATO–PRT exposure, while incubation with either ATO or PRT alone showed smaller or no increases. Higher ROS levels in cells exposed to ATO–PRT correlated with the potentiating effect of PRT to ATO cytotoxicity, although the observed increases may not sufficiently explain the quantitative differences in cell death induction. In the K562 cell line which was resistant to ATO–PRT combinations, these drugs did not increase ROS content. In contrast, elevated ROS levels were found in all cell lines during the first 6 h when ATO, PRT and BSO were combined. Concurrent with increased ROS levels, exposure to ATO–PRT–BSO dramatically decreased intracellular GSH content. Already

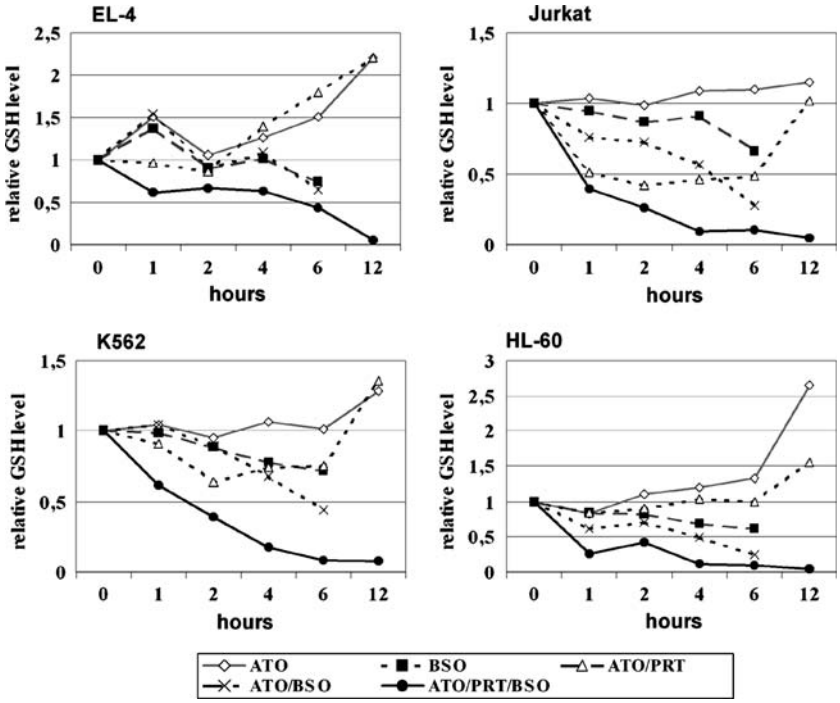

Fig. 7 Relative GSH levels during the first 12 h of drug treatment. Cells were incubated with the indicated drug combinations (2.5 μM ATO; 10 μM PRT; 12.5 μM BSO) and GSH content was determined. Results are shown relative to untreated control cells

after one hour of incubation with the triple combination, the GSH level was reduced by 60% in HL-60 and Jurkat cell lines, and by about 40% in K562 and EL-4. This rapid decrease of GSH content might not be solely due to inhibition of GSH synthesis, but to non-oxidative loss of glutathione in stress-induced apoptosis via GSH extrusion. Apoptotic GSH extrusion was suggested to trigger the downstream events of apoptosis by leaving cells unprotected against thiol oxidation and free radical production [4, 9].

Apoptosis is a well-organised, controlled process consisting of several clearly defined steps including death receptor engagement and/or mitochondrial changes, caspase activation, nuclear condensation and fragmentation, DNA degradation and generation of apoptotic bodies. Several of these steps require hydrolysis of ATP [6], and death signals in the absence of ATP promote necrosis instead of apoptosis [25]. It was described previously that the reduction of GSH levels by BSO augmented cell death via a necrotic rather than an apoptotic process [32]. In our experiments, inclusion of BSO in the treatment modalities changed the cell-death characteristics in a similar way. While in combinations containing ATO and BSO early apoptotic events were still detected, late stages of apoptosis like fragmentation of nuclei and DNA fragmentation were not observed. Measurement of ATP levels confirmed that intracellular ATP fell below 50 and 25% of controls during the first 6 and 12 h of drug treatment, respectively. The only exception was K562, which kept the ATP level at 70% of control. The observed loss of ATP explains the switch from apoptotic to necrotic cell death. A therapy based on the new combination might benefit from this shift for two reasons: first, many cancer cells develop anti-apoptotic mechanisms and escape chemotherapy. Inducing necrosis instead of apoptosis might evade such escape mechanisms. Second, necrosis is known to be immunogenic in contrast to apoptosis, which often is not [43]. Induction of immunogenic responses may help to completely clear the body from malignant cells.

For each of the four cell lines, a similar chronology was observed for the events during incubation with the triple drug combination (Fig. 8). During the first 1–4 h a dramatic loss of GSH took place leaving the cells unprotected towards oxidative stress. In parallel to and following GSH depletion, increased levels of ROS were measured mainly between 4 and 6 h. During the next 6 h, the energy metabolism of the cells was shut down and ATP levels dropped, leading to inhibition of the ATP-dependent steps of apoptosis. Finally, necrotic cell death occured after 12–24 h of drug exposure. The most pronounced increase in ROS levels was observed in HL-60 cells (almost 300% of control) and correlated with an earlier cell death (up to 80% dead cells after 12 h).

It has been demonstrated for many different cell types that the mechanism of ATO-mediated cytoxicity depends on oxidative damage caused by increasing ROS levels. Moderate oxidative stress may elicit protecting responses like a raise of GSH levels and expression of anti-oxidant

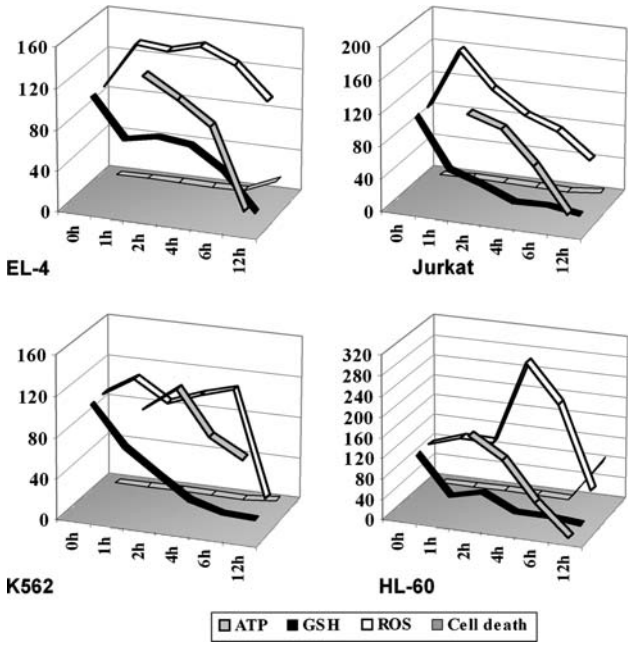

Fig. 8 Summary of ATO–PRT–BSO effects on cellular parameters. For each of the four cell lines tested, the effects caused by the combined treatment with ATO, PRT and BSO (2.5, 10 and 12.5 μM, respectively) during the first hours after drug addition are summarised. For each cell line the loss of GSH preceded an increase in ROS levels. Subsequently, ATP levels dropped and finally cell death occurred, which at 12 h is only visible for EL-4 and HL-60 cells

enzymes which is in part controlled by NF-κB activity [8, 20]. If these cellular rescue mechanisms are simultaneously inhibited by PRT and BSO, the cells are left unprotected to steadily growing oxidative stress and finally undergo cell death. Some enzymes of glycolytic pathways, like glyceraldehyde-3-phosphate dehydrogenase [30] and pyruvate dehydrogenase [26] are sensitive to oxidative damage. By their inactivation, oxidative stress could impair cellular energy production resulting in low ATP levels and necrotic cell death. Cancer cells are known to be more dependent on the glycolytic pathway for ATP generation and shutting down glycolysis is a recognised way to selectively target cancer cells [24]. This may partially explain the observed selectivity of ATO–PRT–BSO death induction for leukemic cells while healthy donor lymphocytes were spared.

In conclusion, the triple combination of ATO, PRT and BSO was shown to kill cells from eight different leukemic cell lines in vitro with very high efficiency. Identically treated HDL were almost unaffected, thus opening an exciting therapeutic option. Evidence was provided that the combinatorial treatment shifted the cell-death response towards necrosis thereby maybe overcoming apoptosis resistance which is a common feature of all established cancer cells. Specific inhibition of cellular rescue mechanisms, which are elicited by the drug treatment, increases drug efficiency and might be considered as a principle with broad practicability.

Acknowledgments This work was supported by the Nofer Institute of Occupational Medicine, Grant No. IMP1.7/2006, and by the Marie Curie Transfer of Knowledge Program "EpiTok" No. 6PR/2004/509829. We specifically thank Drs. Waldek Wagner and Jarosław Dastych for their great support at the flow cytometry laboratory.

References

1. Aggarwal BB (2004) Nuclear factor-kappaB, the enemy within. Cancer Cell 6:203–208
2. Chou WC, Jie C, Kenedy AA, Jones RJ, Trush MA, Dang CV (2004) Role of NADPH oxidase in arsenic-induced reactive oxygen species formation and cytotoxicity in myeloid leukemia cells. Proc Natl Acad Sci USA 101:4578–4583
3. D'Alessio M, Cerella C, De Nicola M, Bergamaschi A, Magrini A, Gualandi G, Alfonsi AM, Ghibelli L (2003) Apoptotic GSH extrusion is associated with free radical generation. Ann NY Acad Sci 1010:449–452
4. Dai J, Weinberg RS, Waxman S, Jing Y (1999) Malignant cells can be sensitized to undergo growth inhibition and apoptosis by arsenic trioxide through modulation of the glutathione redox system. Blood 93:268–277
5. Davison K, Côté S, Mader S, Miller WH (2003) Glutathione depletion overcomes resistance to arsenic trioxide in arsenic-resistant cell lines. Leukemia 17:931–940
6. Eguchi Y, Srinivasan A, Tomaselli KJ, Shimizu S, Tsujimoto Y (1999) ATP-dependent steps in apoptotic signal transduction. Cancer Res 59:2174–2181
7. Felix K, Manna SK, Wise K, Barr J, Ramesh GT (2005) Low level of arsenite activates nuclear factor-kappaB and activator protein-1 in immortalized mesencephalic cells. J Biochem Mol Tox 19:67–77
8. Filomeni G, Aquilano K, Rotilio G, Ciriolo MR (2005) Antiapoptotic response to induced GSH depletion: involvement of heat shock proteins and NF-kappaB activation. Antioxid Redox Signal 7:446–455
9. Ghibelli L, Coppola S, Rotilio G, Lafavia E, Maresca V, Ciriolo MR (1995) Non-oxidative loss of glutathione in apoptosis via GSH extrusion. Biochem Biophys Res Commun 216:313–320
10. Gong J, Traganos F, Darzynkiewicz Z (1994) A selective procedure for DNA extraction from apoptotic cells applicable for gel electrophoresis and flow cytometry. Anal Biochem 218:314–319
11. Gupta S, Yel L, Kim D, Kim C, Chiplunkar S, Gollapudi S (2003) Arsenic trioxide induces apoptosis in peripheral blood T lymphocyte subsets by inducing oxidative stress: a role of Bcl-2. Mol Cancer Ther 2:711–719
12. Han SS, Kim K, Hahm ER, Park CH, Kimler BF, Lee SJ, Kim WS, Jung CW, Park K, Kim J, Yoon SS, Lee JH, Park S (2005) Arsenic trioxide represses constitutive activation of NF-kappaB and COX-2 expression in human acute myeloid leukemia, HL-60. J Cell Biochem 94:695–707
13. Hu XM, Hirano T, Oka K (2003) Arsenic trioxide induces apoptosis in cells of MOLT-4 and its daunorubicin-resistant cell line via depletion of intracellular glutathione, disruption of mitochondrial membrane potential and activation of caspase-3. Cancer Chemother Pharmacol 52:47–58
14. Jing Y, Dai J, Chalmers-Redman RM, Tatton WG, Waxman S (1999) Arsenic trioxide selectively induces acute promyelocytic leukemia cell apoptosis via a hydrogen peroxide-dependent pathway. Blood 94:2102–2111

15. Kapahi P, Takahashi T, Natoli G, Adams SR, Chen Y, Tsien RY, Karin M (2000) Inhibition of NF-kappa B activation by arsenite through reaction with a critical cysteine in the activation loop of Ikappa B kinase. J Biol Chem 275:36062–36066
16. Karin M (2006) Nuclear factor-kappaB in cancer development and progression. Nature 441:431–436
17. Kerbauy DM, Lesnikov V, Abbasi N, Seal S, Scott B, Deeg HJ (2005) NF-kB and FLIP in arsenic trioxide (ATO)–induced apoptosis in myelodysplastic syndromes (MDSs). Blood 106:3917–3925
18. Kwok BH, Koh B, Ndubuisi MI, Elofsson M, Crews CM (2001) The anti-inflammatory natural product parthenolide from the medicinal herb Feverfew directly binds to and inhibits IkappaB kinase. Chem Biol 8:759–766
19. Lemarie A, Morzadec C, Merino D, Micheau O, Fardel O, Vernhet L (2006) Arsenic trioxide induces apoptosis of human monocytes during macrophagic differentiation through nuclear factor-kappaB-related survival pathway down-regulation. J Pharmacol Exp Ther 316:304–314
20. Li M, Cai JF, Chiu JF (2002) Arsenic induces oxidative stress and activates stress gene expressions in cultured lung epithelial cells. J Cell Biochem 87:29–38
21. Maeda H, Hori S, Ohizumi H, Segawa T, Kakehi Y, Ogawa O, Kakizuka A (2004) Effective treatment of advanced solid tumors by the combination of arsenic trioxide and L-buthionine-sulfoximine. Cell Death Diff 11:737–746
22. Mathas S, Lietz A, Janz M, Hinz M, Jundt F, Scheidereit C, Bommert K, Dorken B (2003) Inhibition of NF-κB essentially contributes to arsenic-induced apoptosis. Blood 102:1028–1034
23. Nakshatri H, Rice SE, Bhat-Nakshatri P (2004) Antitumor agent parthenolide reverses resistance of breast cancer cells to tumor necrosis factor-related apoptosis-inducing ligand through sustained activation of c-Jun N-terminal kinase. Oncogene 23:7330–7344
24. Pelicano H, Martin DS, Xu R-H, Huang P (2006) Glycolysis inhibition for anticancer treatment. Oncogene 25:4633–4646
25. Saito Y, Nishio K, Ogawa Y, Kimata J, Kinumi T, Yoshida Y, Noguchi N, Niki E (2006) Turning point in apoptosis/necrosis induced by hydrogen peroxide. Free Radic Res 40:619–630
26. Samikkannu T, Chen CH, Yih LH, Wang AS, Lin SY, Chen TC, Jan KY (2003) Reactive oxygen species are involved in arsenic trioxide inhibition of pyruvate dehydrogenase activity. Chem Res Toxicol 16:409–414
27. Seo T, Urasaki Y, Takemura H, Ueda T (2005) Arsenic trioxide circumvents multidrug resistance based on different mechanisms in human leukemia cell lines. Anticancer Res 25:991–998
28. Shen ZX, Chen GQ, Ni JH, Li XS, Xiong SM, Qiu QY, Zhu J, Tang W, Sun GL, Yang KQ, Chen Y, Zhou L, Fang ZW, Wang YT, Ma J, Zhang P, Zhang TD, Chen SJ, Chen Z, Wang ZY (1997) Use of arsenic trioxide (As_2O_3) in the treatment of acute promyelocytic leukemia (APL): II. Clinical efficacy and pharmacokinetics in relapsed patients. Blood 89:3354–3360
29. Steele AJ, Jones DT, Ganeshaguru K, Duke VM, Yogashangary BC, North JM, Lowdell MW, Kottaridis PD, Mehta AB, Prentice AG, Hoffbrand AV, Wickremasinghe RG (2006) The sesquiterpene lactone parthenolide induces selective apoptosis of B-chronic lymphocytic leukemia cells in vitro. Leukemia 20:1073–1079
30. Sukhanov S, Higashi Y, Shai SY, Itabe H, Ono K, Parthasarathy S, Delafontaine P (2006) Novel effect of oxidized low-density lipoprotein. Cellular ATP depletion via downregulation of Glyceraldehyde-3-Phosphate dehydrogenase. Circ Res 99:191–200
31. Tabellini G, Cappellini A, Tazzari PL, Fala F, Billi AM, Manzoli L, Cocco L, Martelli AM (2005) Phosphoinositide 3-kinase/Akt involvement in arsenic trioxide resistance of human leukemia cells. J Cell Physiol 202:623–634
32. Troyano A, Sancho P, Fernandez C, de Blas E, Bernardi P, Aller P (2003) The selection between apoptosis and necrosis is differentially regulated in hydrogen peroxide-treated and glutathione-depleted human promonocytic cells. Cell Death Diff 10:889–898
33. Turco MC, Romano MF, Petrella A, Bisogni R, Tassone P, Venuta S (2004) NF-kappaB/Rel-mediated regulation of apoptosis in hematologic malignancies and normal hematopoietic progenitors. Leukemia 18:11–17
34. Verstovsek S, Giles F, Quinta's-Cardama A, Perez N, Ravandi-Kashani F, Beran M, Freireich E, Kantarjian H (2006) Arsenic derivatives in hematologic malignancies, a role beyond acute promyelocytic leukemia? Hematol Oncol 24:181–188
35. Wang W, Adachi M, Kawamura R, Sakamoto H, Hayashi T, Ishida T, Imai K, Shinomura Y (2006) Parthenolide-induced apoptosis in multiple myeloma cells involves reactive oxygen species generation and cell sensitivity depends on catalase activity. Apoptosis 11:2225–2235
36. Woo SH, Park IC, Park MJ, An S, Lee HC, Jin HO, Park SA, Cho H, Lee SJ, Gwak HS, Hong YJ, Hong SI, Rhee CH (2004) Arsenic trioxide sensitizes CD95/Fas-induced apoptosis through ROS-mediated upregulation of CD95/Fas by NF-kappaB activation. Int J Cancer 112:596–606
37. Yang CH, Kuo ML, Chen JC, Chen YC (1999) Arsenic trioxide sensitivity is associated with low level of glutathione in cancer cells. Br J Cancer 81:796–799
38. Yi J, Gao F, Shi G, Li H, Wang Z, Shi X, Tang X (2002) The inherent cellular level of reactive oxygen species: one of the mechanisms determining apoptotic susceptibility of leukemic cells to arsenic trioxide. Apoptosis 7:209–215
39. Zhang S, Lin ZN, Yang CF, Shi X, Ong CN, Shen HM (2004) Suppressed NF-kappaB and sustained JNK activation contribute to the sensitization effect of parthenolide to TNF-alpha-induced apoptosis in human cancer cells. Carcinogenesis 25:2191–2199
40. Zhang S, Ong CN, Shen HM (2004) Critical roles of intracellular thiols and calcium in parthenolide-induced apoptosis in human colorectal cancer cells. Cancer Lett 208:143–153
41. Zhou L, Jing Y, Styblo M, Chen Z, Waxman S (2005) Glutathione-S-transferase pi inhibits As2O3-induced apoptosis in lymphoma cells: involvement of hydrogen peroxide catabolism. Blood 105:1198–1203
42. Zhu XH, Shen YL, Jing YK, Cai X, Jia PM, Huang Y, Tang W, Shi GY, Sun YP, Dai J, Wang ZY, Chen SJ, Zhang TD, Waxman S, Chen Z, Chen GQ (1999) Apoptosis and growth inhibition in malignant lymphocytes after treatment with arsenic trioxide at clinically achievable concentrations. J Natl Cancer Inst 91: 772–778
43. Zitvogel L, Tesniere A, Kroemer G (2006) Cancer despite immunosurveillance, immunoselection and immunosubversion. Nat Rev Immunol 6:715–727